PL-TR-94-2313

IR Reflectance of Aircraft Paints

Brian P. Sandford

2 December 1985

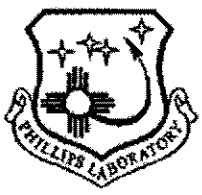

PHILLIPS LABORATORY
Directorate of Geophysics
AIR FORCE MATERIEL COMMAND
HANSCOM AIR FORCE BASE, MA 01731-3010

REPORT DOCUMENTATION PAGE

Form Approved
OMB No. 0704-01-0188

PLEASE DO NOT RETURN YOUR FORM TO THE ABOVE ADDRESS.

1. REPORT DATE *(DD-MM-YYYY)*	2. REPORT TYPE	3. DATES COVERED *(From - To)*
12-02-1985	Scientific, Final	

4. TITLE AND SUBTITLE
Infrared Reflectance of Aircraft Paints

5a. CONTRACT NUMBER

5b. GRANT NUMBER

5c. PROGRAM ELEMENT NUMBER
62601F

6. AUTHORS
Brian P. Sandford

5d. PROJECT NUMBER
3054

5e. TASK NUMBER
02

5f. WORK UNIT NUMBER
01

7. PERFORMING ORGANIZATION NAME(S) AND ADDRESS(ES)

Phillips Laboratory
29 Randolph Road
Hanscom AFB, MA 01731-3010

8. PERFORMING ORGANIZATION REPORT NUMBER
PL-TR-94-2313

9. SPONSORING/MONITORING AGENCY NAME(S) AND ADDRESS(ES)
Defense Advanced Research Projects Agency (STO)
1400 Wilson Blvd
Arlington, VA 22209

10. SPONSOR/MONITOR'S ACRONYM(S)
PL/GPOA

11. SPONSOR/MONITOR'S REPORT NUMBER(S)

12. DISTRIBUTION/AVAILABILITY STATEMENT
Approved for Public Release; distribution unlimited.

13. SUPPLEMENTARY NOTES
Publicly Releasable Revision to AFGL-TR-84-0307

14. ABSTRACT

The reflectance and emittance properties of aircraft paints play an important role in determining IR contrast signatures. As an adjunct to its aircraft signature measurement program, the Geophysics Directorate of the Phillips Laboratory has also obtained paint chips from operational aircraft and had Surface Optics Corp. measure the paint directional and bidirectional reflectance properties. This report presents samples of these data and shows how they can be incorporated into aircraft signature calculations through of a semi-empirical bidirectional reflectance model. The model is incorporated into aircraft signature calculations through use of a semi-empirical bidirectional reflectance model. The model is incorporated into an IR signature code that calculates target thermal emissions plus specular and diffuse scatter of sunshine, earthshine, and skyshine.

15. SUBJECT TERMS
Spectral directional reflectance
Bidirectional reflectance

16. SECURITY CLASSIFICATION OF:			17. LIMITATION OF ABSTRACT	18. NUMBER OF PAGES	19a. NAME OF RESPONSIBLE PERSON
a. REPORT	b. ABSTRACT	c. THIS PAGE			Brian P. Sandford
UNCL	UNCL	UNCL	UNL	28	19B. TELEPHONE NUMBER *(Include area code)*

Contents

Illustrations

INFRARED REFLECTANCE PROPERTIES OF AIRCRAFT PAINTS

12 February 1985
(Revised August 1994)

Brian P. Sandford
Phillips Laboratory, Geophysics Directorate/GPOA
29 Randolph Road
Hanscom AFB, MA 01731-3010
and

David C. Robertson
Spectral Sciences, Inc.
99 S. Bedford Street
Burlington, MA 01803-5169

ABSTRACT

The reflectance and emittance properties of aircraft paints play an important role in determining IR contrast signatures. As an adjunct to its aircraft signature measurement program, the Geophysics Directorate of the Phillips Laboratory has also obtained paint chips from operational aircraft and had Surface Optics, Corp. measure the paint directional and bidirectional reflectance properties. This paper presents samples of these data and shows how they can be incorporated into aircraft signature calculations through use of a semi-empirical bidirectional reflectance model. The model is incorporated into an IR signature code that calculates target thermal emissions plus specular and diffuse scatter of sunshine, earthshine and skyshine.

1. INTRODUCTION

Analysis of elements contributing to aircraft signatures in the infrared (IR) has become of increasing importance as IR detectors make rapid gains in efficiency and sensitivity. The increased sophistication of air defense systems is forcing aircraft designers to pay careful attention to observable features throughout the electromagnetic spectrum. Since the IR plays an important role for many present and proposed systems, reflections and emissions from the airframe can lead to vulnerable situations if not considered during their design.

Except for molecular emissions of the exhaust plume and emissions from hot metal parts related to the engine, radiation emitted and scattered by the airframe is the dominant part of the aircraft IR signature. The magnitudes of the airframe components are largely governed by the emissive-reflective properties of the surface coatings, i.e., paints. This paper presents a discussion of the emissive-reflective characteristics of paints from operational aircraft by describing a database developed by the Air Force Phillips Laboratory, Geophysics Directorate (PL/GPOA) and a semi-empirical reflectance model developed by Spectral Sciences, Inc. (SSI).

The airframe contrast signature in the IR consists of skin thermal emission plus reflection of sunshine, skyshine, and earthshine. The intensities of these signature components can be characterized from the directional and bidirectional reflectance of the surface. These are well defined optical surface properties that can be measured in the laboratory and then incorporated into an aircraft signature computer code. The next section presents the nomenclature for describing the optical properties of the surface. Section 3 presents illustrative examples of the database developed by PL/GPOA from measurements by Surface Optics, Corp.[1-3] (SOC). Section 4 describes an emission-reflection model which derives its parameters from the data and has been incorporated into SPIRITS and other aircraft signature codes.[4]

2. GENERAL REFLECTANCE PARAMETERS

The optical properties of a surface are completely defined by the bidirectional reflectance distribution function (BRDF). The BRDF is defined as the surface reflectance for a given wavelength (λ), angles of incidence (θ_i,φ_i) and angles of reflectance (θ_r,φ_r). The angles (θ,φ), shown in Figure 1, are the standard zenith and polar angles measured from the z and x axes, respectively. Reflectance parameters used in this paper are given in Table 1. This list is based on recent definitions that should be used in order to standardize the nomenclature.[5,6] For an exhaustive discussion of this issue, the reader is directed to Reference (6). The wavelength dependence of the BRDF is an important function that has been suppressed in this treatment solely to simplify the notation.

When the surface shows no preferentially oriented marks (striae), the number of angles in the BRDF may be reduced to three by defining the incident azimuth angle (φ_{r_r}) relative to φ_i. The unit of bidirectional reflectance is sr^{-1}; it is defined as the ratio of the reflected intensity ($W.sr^{-1}$) in direction (θ_r,φ_r) to the incident energy in a collimated beam that illuminates the surface from direction (θ_i,φ_i).

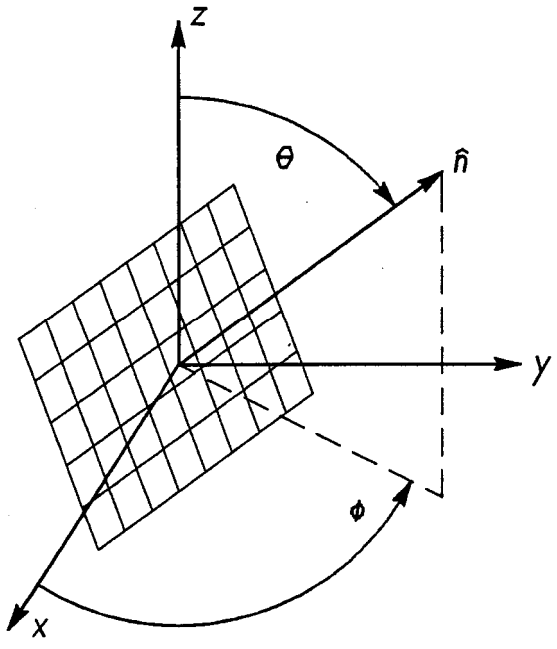

Figure 1. Definition of the Angles (θ,φ).

Table 1. Nomenclature List for Various Reflectance Quantities.

SYMBOL	DEFINITION	UNITS
$\rho,\rho(\lambda)$	(spectral) surface reflectance	-
$\rho(\lambda,\theta)$	directional spectral reflectance	-
$\varepsilon,\varepsilon(\lambda)$	(spectral) surface emittance	-
$\varepsilon(\lambda,\theta)$	directional spectral emittance	-
$\alpha,\alpha(\lambda)$	(spectral) surface absorptivity	-
α	angle between glint vector and surface normal	rad.
A	area	m^2
E	irradiance (replaces H)	$W \bullet m^{-2}$
$f_r,f_r(\theta_i,\varphi_i;\theta_r,\varphi_r)$	BRDF Bi-directional Reflectance Distribution Function	sr^{-1}
f_d,f_s	diffuse, specular part of the spectral BRDF	-
f_{rI}	BRIDF Bi-directional reflected intensity distribution function	sr^{-1}
I	source radiant intensity (replaces J)	$W \bullet sr^{-1}$
L	radiance (replaces N)	$W \bullet m^{-2} \bullet sr^{-1}$

Surfaces are frequently described as near diffuse (flat surface) or near specular (mirror surface). A perfectly diffuse or lambertian surface reflects energy isotropically, i.e., the reflected energy measured in any direction in the same for a given incident ray. Since the intercepted energy depends only on the angle of incidence (θ_i) and the sample area, the BRDF is independent of (θ_r,φ_r). A 100 percent reflecting and perfectly diffuse sample has, for all incident angles, a BRDF of $1/\pi$ sr^{-1} in all directions. A specular surface reflects energy according to Snell's law, i.e., the incident beam is reflected with angle $\theta_r = \theta_i$ and $\varphi_r = \varphi_i + 180°$. A perfectly reflecting specular surface sends all the incident beam energy into the reflected beam with no loss in intensity. If the incident beam were perfectly collimated (a physical impossibility), the BRDF would be infinite at the reflected ray (θ_r,φ_r) and zero at all other angles (i.e., a delta-function). Actual paint samples invariably exhibit features that are neither perfectly lambertain nor perfectly specular.

When the BRDF is integrated over the hemisphere above the sample, the directional reflectance is obtained. The directional reflectance (ρ) is only a function of the angles of incidence (θ_i,φ_i) and reduces to a function of just θ_i when the surface is homogeneous with no preferential marks or surface scratches. The integral relating directional and bidirectional reflectance is

$$\rho = \int f_r(\theta_i,\phi_i;\theta_r,\phi_r)\, d\omega_r \qquad (1)$$

Conservation of energy requires that radiation incident on a surface be either absorbed, transmitted or reflected. This requires that

$$\alpha + \tau + \rho = 1 \quad , \tag{2}$$

where α, τ, ρ are the absorptivity, transmittance, and reflectance. This is also true for the spectral quantities. Excepting transparent surfaces like aircraft canopies, surfaces are opaque, and $\tau(\lambda) = 0$. Thus,

$$\alpha(\lambda) + \rho(\lambda) = 1 \quad . \tag{3}$$

Note that Equations (2) and (3) are not always valid for each of the polarization components.[5] Kirchhoff's law states that the absorptivity and emissivity of a blackbody in thermal equilibrium are equal.[6] This is valid totally and spectrally,[5] i.e.,

$$\alpha = \epsilon \quad \text{and} \quad \alpha(\lambda) = \epsilon(\lambda) \quad . \tag{4}$$

This assumption relates the absorption of incident radiation at a given angle, (θ_i,φ_i), to the directional emissivity at that angle.

2.1 Viewing Geometry

Consider a planar surface element of area A. Its orientation in space is specified by the polar angles (θ,φ) of its normal; θ is measured from the zenith, and φ is measured from the x-axis. The coordinate axes are illustrated in Figure 1. The same coordinate system is used to specify the direction to the observer (θ_r,φ_r) and to the sun (θ_i,φ_i). The unit vectors specifying the directions towards the observer and illumination source are $\hat{o}$ and $\hat{s}$, respectively. Thus, the directions of $\hat{o}$ and $\hat{s}$ are given by (θ_r,φ_r) and (θ_i,φ_i), respectively.

Various angles for defining the scattering geometry are shown in Figure 2. For simplicity, the surface normal $\hat{n}$ lies along the z-axis. The unit vectors $\hat{o}$ and $\hat{s}$ point towards the observer and source, respectively. The glint vector $\hat{g}$ is the unit vector for the bisector of the angle between $\hat{o}$ and $\hat{s}$. It is given by

$$\hat{g} = (\hat{o} + \hat{s}) \,/\, \sqrt{2(1 + \hat{o} \cdot \hat{s})} \quad . \tag{5}$$

The angle α (not shown) is defined as the angle between $\hat{g}$ and the surface normal. It is given by

$$\cos\alpha = \hat{g} \cdot \hat{n} \quad , \tag{6}$$

Where $\hat{n}$ is the direction of the surface normal. Note that $\alpha = 0$ corresponds to maximum specular reflection.

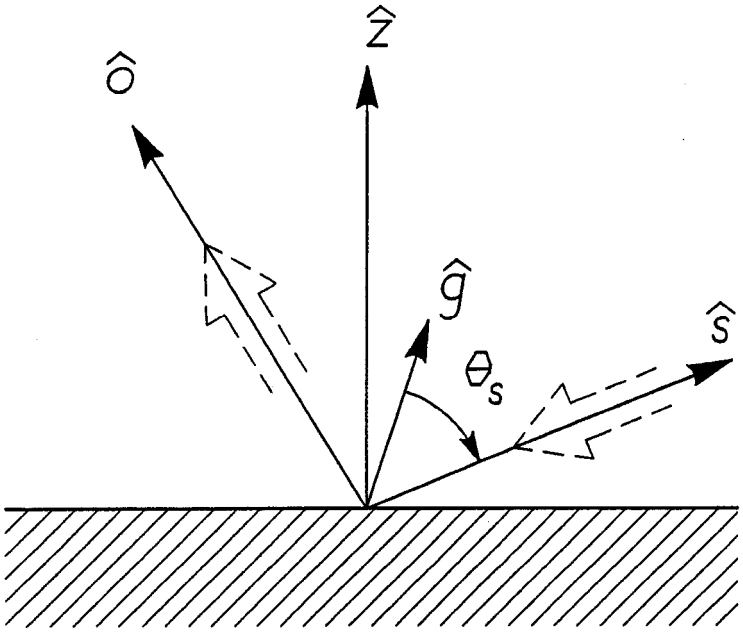

Figure 2. Angles for Scattering by a Surface Element.

3. PAINT REFLECTANCE DATABASE

The PL Flying Infrared Signatures Technology Aircraft (FISTA) has been actively engaged in field measurements (air-air) of aircraft IR signatures. Under many different programs PL/GPOA has supported reduction and analyses of both target and background data. Application of these data to other scenario conditions is made through the use of validated models. An important element is, of course, the properties of airframe surface coatings or paints. The complex phenomenology of operational aircraft finishes is strongly influenced by the spectral reflectance and bidirectional reflectance. Since a database for reflectances of operational aircraft could not be found, PL/GPOA collected samples of panels from various aircraft and contracted to Surface Optics Corporation (SOC), P.O. Box 261602, San Diego, CA 92196, the task of measuring paint reflectance properties. To date 50 (currently 102) samples have been taken, mostly from operational aircraft, and 28 of these have been measured by SOC. Table 2 lists the samples as of February 1985. Later measurements of spectral directional reflectance included the perpendicular and parallel polarizations in addition to their sum. Approximate wavelengths for the BRDF measurements are also given in the table.

3.1 Optical Properties

The measurement techniques used by SOC for the directional reflectance (ρ) and BRDF are described elsewhere,[1-3] so we give only a brief description here. The directional reflectance, $\rho(\theta_i,\varphi_i)$, is a measure of the ratio of the energy reflected into the hemisphere above the sample to the energy incident from a given vector direction. The energy in the incident beam is divided into absorbed and reflected energy without concern for where in the hemisphere the reflected energy goes. This means that a surface can be specular or diffuse and still have the same directional reflectance. Directional reflectance data are required for the determination of thermal emittance and solar absorptance, for thermal balance calculations, and in the establishment of bidirectional reflectance in absolute terms. In many cases the degree of surface specularity is important, and the BRDF is required to describe the distribution of the reflected energy into the hemisphere above the sample. It must be measured over enough points in the upper hemisphere to provide an adequate description of the reflected energy distribution. The number of points depends on whether the surface exhibits a predominately diffuse or specular reflectance characteristic. The BRDF is influenced not only by the composition of the surface material but also by its condition and/or roughness.

Table 2. Aircraft Paint Samples at PL/GPOA.

Sample Number AFGL	Sample Number ERAS	Descriptions	Reflectance Polarization	Brdf Wavelength (μm)
1	FS3411	Flat blue	U	4, 10
2	FS3483	Semi gloss white	P	4, 10
3	FS3461	High gloss white	U	4, 10
4	FS3412	Flat metalized gray	U	4, 10
5	FS3484	Anodized aluminum	P	4, 10
6	FS3485	Semi gloss light gray	P	4, 10
7	-	Flat deep green	-	-
8	FS3462	High gloss light gray	U	4, 10
9	FS3463	Flat brown	U	4, 10
10	FS3464	High gloss white	U	4, 10
11	FS3465	Flat dark green	U	4, 10
12	FS3413	Flat gray on steel	U	-
13	FS3414	Semi gloss olive	U	-
14	FS3415	Semi gloss gray	U	-
15	FS3416	Semi gloss olive green	U	-
16	FS3417	High gloss white	U	-
17	FS3486	Flat dark gray	P	4, 10
18	FS3487	High gloss gray	P	4, 10
19	-	High gloss white	-	-
20	FS3488	Semi gloss blue/green	P	4, 10
21	FS3489	Flat orange/brown	P	4, 10
22	FS3490	Semi gloss tan	P	4, 10
23	FS3491	Very flat black	P	4, 10
(24)	FS3492	Gray water base wash (data only)	P	4
25	FS3606	Gloss gray	P	1, 4, 10
26	-	High gloss white	-	-
27	-	High gloss dark gray	-	-
28	FS3607	High gloss white	P	1, 4, 10
29	-	High gloss light gray	-	-
30	-	High gloss light blue	-	-
31	FS3673	High gloss blue	P	1, 4, 10
32	-	Same as 30	-	-
33	-	High gloss dark blue	-	-
34	-	Same as 33	-	-
35	-	Same as 26	-	-
36	-	High gloss white	-	-
37	-	High gloss white	-	-
38	-	Waxed aluminum	P	1, 4, 10
39	-	Same as 29	-	-
40	-	Same as 27	-	-
41	-	Same as 31	-	-
42	-	Gloss medium gray	-	-
43	-	High gloss metalized gold	P	1, 4, 10
44	-	High gloss white	-	-
45	-	High gloss black	P	1, 4, 10
46	-	High gloss red	-	-
47	-	High gloss dark blue	-	-
48	-	High gloss blue	-	-
49	-	Flat gray	-	-
50	-	High gloss light gray	-	-
51	-	High gloss white	-	-

3.1.1 SOC Integrating Sphere

In the wavelength range 0.3 to 2.0 μm, SOC utilizes an integrating sphere with a double beam spectrophotometer to measure directional reflectance. The spectrophotometer provides a continuous spectral directional reflectance output from 0.3 to 2.0 μm. Directional reflectance can also be directly determined at discrete wavelengths by setting the dispersing elements at the desired wavelength. The source is a 200 W (3400 K) lamp and a 150 W xenon lamp that has a continuous output over the desired spectral range. A photodetector is used for 0.3 to 0.6 μm and a PbS detector from 0.6 to 2.0 μm. The internal surface of the nine inch diameter integrating sphere is coated with a thick layer of magnesium oxide. The sample, located at the center of the sphere, and the hemisphere behind it are uniformly illuminated. The instrument utilizes a two beam system; one beam looks at the surface of the sample and the other, the reference or 100 percent beam, looks at the wall of the integrating sphere. The instrument automatically computes and records the ratio of the power incident on the sample surface from the hemispherical uniform source to that reflected in the direction of the receiver (the spectrophotometer). This ratio is the directional reflectance of the sample. The angle at which the directional reflectance is measured is varied by rotating the sample.

Some limitations of the instrument are:

1. Reflections from normal incidence do not include the specular component. Measurements of the directional reflectance at normal incidence with this type of instrument are usually made to determine the ratio of the specular to diffuse components of the reflectance by comparing to a near normal (22°) measurement that has both components.

2. Measurements at "near normal" incidence are limited to an angle of about 20° from the normal.

3. Measurements at "grazing" incidence are limited to an angle of about 80° from the normal. This limitation arises from two considerations. First the image of the spectrometer entrance slit projected to the sample surface falls off the finite sized sample as the sample becomes parallel to the direction of the receiver. Second, as grazing incidence is approached, due care must be taken to assure the energy is in fact not reflected from the edge of the sample.

3.1.2 SOC Ellipsoidal Reflectometer

Suitable materials are not available for integrating spheres over such a wide IR spectral range, so an ellipsoidal reflectometer is used to measure the directional reflectance from 1.0 to 600 μm.[1,3] This instrument utilizes a blackbody source, a grating spectrometer, filters for wavelength determination and

cryogenically cooled detectors with the source located at one focus and the sample at the other. The focusing characteristic of an ellipsoid with a small eccentricity is such that a point source of light emanating from one focus is imaged at the other. Using a properly sized radiation source, the sample is uniformly illuminated over a hemisphere of 2π sr. Radiation reflected from the sample is collected by a sample mirror above the sample and then reflected by transfer optics into the spectrometers. Different directions are obtained by rotating the hemi-ellipsoid, source and sample with respect to the fixed sample mirror. Reflectance values are obtained by comparison to a known "standard" that is alternately measured along with the sample at each wavelength and direction.

Like the integrating sphere, this instrument too has limitations:

1. Measurements at normal incidence do not contain the specular component because the incident specular component is blocked from reaching the sample by the sample mirror.

2. Measurements at “near normal” incidence are limited to an angle of 18° from the normal. This limitation is fixed by the size of the sample mirror and the geometry of the system.

3. Measurements at “grazing” incidence are limited to an angle of about 75° from the normal for exactly the same reasons given above for the integrating sphere.

3.1.3 Bidirectional Reflectance Measurements

The BRDF is measured by placing a (known) source at (θ_i,φ_i=0) and a sensor at (θ_r,φ_r). In the visible wavelength region, tungsten lamp sources and photodetectors are employed; in the IR region a blackbody source and cryogenically cooled detectors are used. Wavelength determination is obtained by means of narrow band filters. The reflective BRDF is measured at a closely spaced positions (θ_r,φ_r) over a range of incident angles (θ_i). When samples are isotropic about their normals, it is not necessary to vary the incident azimuth (φ_i). If the sample has surface structure that exhibits a preferred (as opposed to random) direction, the BRDF may vary significantly as a function of (φ_i); in this case BRDF measurements at several incident azimuth angles are required to fully characterize such a sample.

The discrete values of a relative BRDF serve to characterize the reflectance of the sample. These relative BRDFs are then summed (integrated) and equated to the directional reflectance measured at the same incidence angle θ_i. This yields as absolute BRDF. In making the measurements, the sample is over-illuminated and over-detected. A chopper and synchronous amplifier are used to remove stray energy effects and to improve signal-to-noise ratio, a very important consideration in the far infrared. This also eliminates thermal emissions by the sample at the longer wavelengths.

Measurement limitations of this BRDF apparatus are:

1. True monostatic measurements cannot be made with this type of bidirectional reflectance apparatus. The source and detector cannot be brought into coincidence either mechanically or optically. In the visible and near IR spectrum, the detector-source included angle may be reduced to a minimum of about 15°. In the far IR, this angle is limited to a minimum of about 30° because of the physical size of the detector dewar.

2. BRDF measurements are limited to grazing angles of about 85°.

3. Very "black" samples, specular or diffuse, can yield noisy bidirectional reflectance data because the signal-to-noise ratio attainable with the apparatus is low.

4. The bidirectional reflectance in the grazing angles between 85° and 90° may include a significant portion of the reflected energy, which amount is difficult to estimate by extrapolation. The calibration of relative BRDF to absolute BRDF is done by normalizing to the directional reflectance; this can give rise to an error of up to 5 percent.

3.1.4 Sample Preparation

Skin samples were collected from operational aircraft, either from recently crashed aircraft or from small inspection covers that could easily be replaced. The covers were checked to insure that their surface finishes were typical of the finish and condition of that paint on the aircraft as a whole. In all cases, the coatings have been subjected to normal operational conditions, that is, they have been exposed to weather, repairs, retouching, cleaning, flying, and handling that arises during a typical lifetime in service.

The SOC equipment described above for directional reflectance and BRDF measurements utilized the same size and type sample. This feature was purposely designed into the apparatus to assure that identical samples may be used for both measurements. This is especially important for the BRDF since its normalization requires use of the directional reflectance results. The samples are one inch flat discs that were milled by PL/GPOA from the aircraft skin samples, with the outer rim under cut at a sharp angle to minimize edge reflection.

Samples were measured “as received” and in a cleaned condition. Cleaning increased the reflectivity by only a few percent at most. These samples were recleaned by gently scrubbing with an aircraft cleaning detergent, thoroughly rinsing under running tap water, blotting off excess water with paper towels and allowed to air dry. This process is similar to that used to clean aircraft under operational conditions.

3.2 Paint Reflectance Data

Properties of twelve illustrative paint samples are tabulated in Table 3. The table also includes the Expanded Retrieval Analysis System (ERAS)[1] sample numbers, color, visible surface character, width of the specular glint lobe at a 4 and 10 μm, and solar absorptance. All substrates are aluminum, and all finishes are paint.

The samples at PL/GPOA cover a wide range of paints from very glossy surfaces with surface structure scale sizes much less than 1 μm on samples AFGL-08 and -18 to a very diffuse surface with surface structure scale size about 20 μm on sample AFGL-23. The former cases exhibit strong specular reflectance at all IR and visible wavelengths while the latter case is an almost perfect Lambertain surface out to at least 14 μm. Most other samples exhibit a combination of specular and diffuse characteristics. Paints like sample AFGL-17 appear flat in the visible but exhibit a high degree of specularity in the LWIR and are typical of camouflage paints currently used on aircraft. The IR reflectance at wavelengths greater than 3 μm where a paint binder becomes opaque is independent of a sample's color; it appears to depend almost totally on the surface roughness, most likely because the binders for these paints are similar.

Table 3. Summary of Paint Sample Properties.

Sample #		Color	Surface Description	*Glint lobe		Solar
AFGL	ERAS					Absorption
1	FS3411	Blue	Slight sheet	24.	5.	0.77
2	FS3483	White	Moderate sheen	3.	3.	0.40
3	FS3461	White	High gloss	3.5	2.3	0.29
4	FS3412	Gray	No sheen (metalized)	Diffuse		0.70
6	FS3485	Lt. gray	Semi gloss	2.3	3.	0.70
8	FS3462	Lt. gray	High gloss	3.5	4.5	0.69
9	FS3463	Brown	Flat (almost no sheen)	31.	21.	0.83
10	FS3464	White	High gloss	3.	3.5	0.26
11	FS3465	Dk. green	Flat (almost no sheen)	11.	7.	0.92
17	FS3486	Dk. gray	Flat	55.	6.5	0.85
18	FS3487	Gray	High gloss	3.	3.	0.69
23	FS3491	Black	Very flat (Nextlel suede)	Diffuse		0.97

*Glint lobe width in degrees at half peak reflectance at 40° incidence angle.

Examples of the SOC reflectance data are given for three samples, AFGL-01, -03, and -09. The overall texture of AFGL-01 has a grain structure of less than 10 μm with a dull finish to the eye, and the paint is underlaid by a few small bumps that look like dust particles under the top coat. There are two small scratches that do not penetrate the top coat. At near specular angles in the visible, it exhibits a slight sheen, and under a microscope very small centers in the paint appear to be highly reflective. As an example of BRDF plots, AFGL-01 is shown in Figure 3.

The unpolarized directional reflectance, $\rho(\lambda,\theta)$, of AFGL-03 and -09 are shown in Figure 4 for the 0.3 - 25 μm spectral region. The dip around 3 μm is characteristic of many of these samples and is most likely due to absorption by a C-II methyl bond in the paint binder. Sample AFGL-03 is a high gloss white paint, and AFGL-09 is a flat brown paint. Although different in the visible, the samples are similar in the IR (beyond 3 μm). Their directional reflectances at three wavelengths are shown in Figure 5 for radiation incident from 20° to 75°. Figure 6 shows a linear plot of the BRDF for each sample with θ_i=40° and λ=10 μm. Figures 7 and 8 show logarithmic plots of the BRDF for different λ's and θ_i's. The logarithmic plots are more useful than the linear ones in Figure 6 because the intensities of both the specular and diffuse components can be seen. By definition, the illuminating beam has an azimuthal angle φ_i of 0°. The receiver was located at various zenith angles (ρ_r=0, 85°) for three azimuthal angles (φ_r =180, 90, and 0°). Note that the specular lobe is maximum in the plane defined by φ_r=180° (forward scatter).

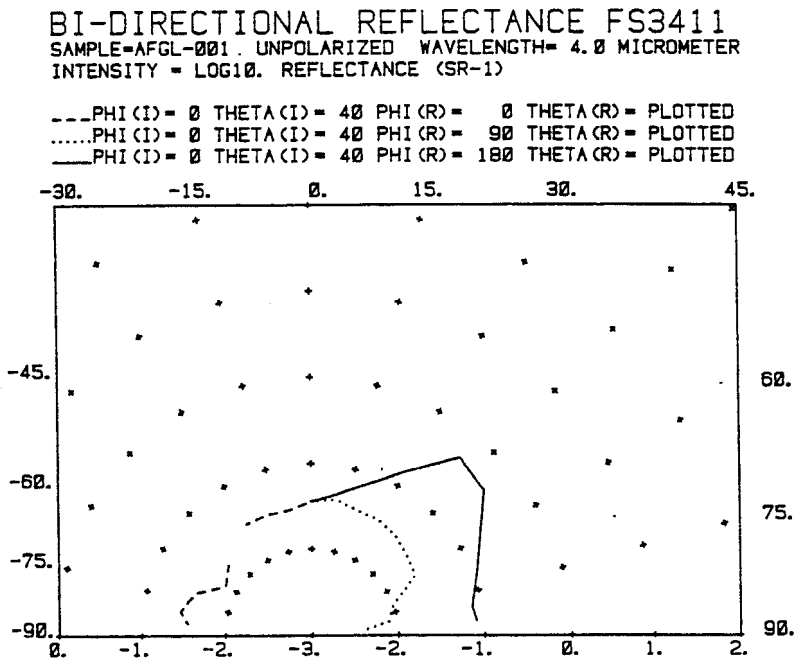

Figure 3. Logarithmic Polar Plot of the BRDF for Sample AFGL-01.

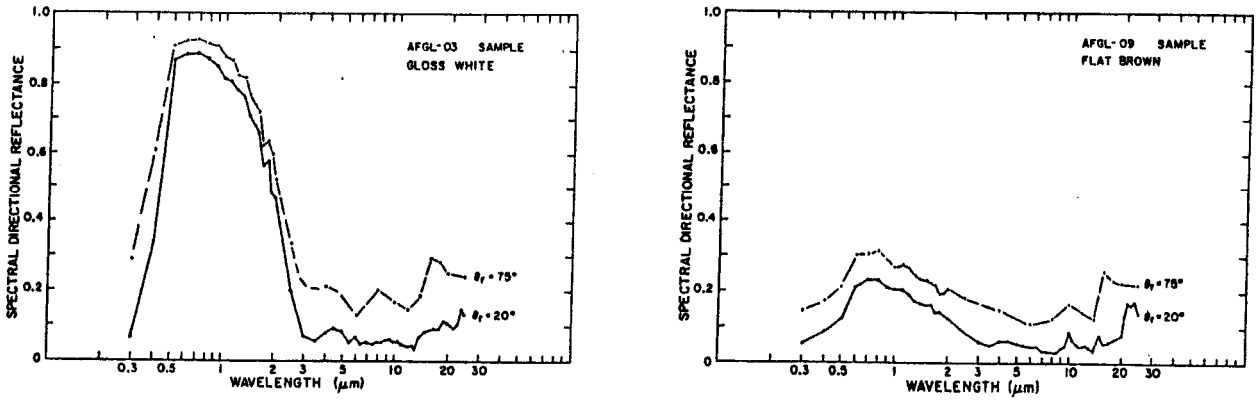

Figure 4. The Spectral Directional Reflectance for Samples AFGL-03 and -09.

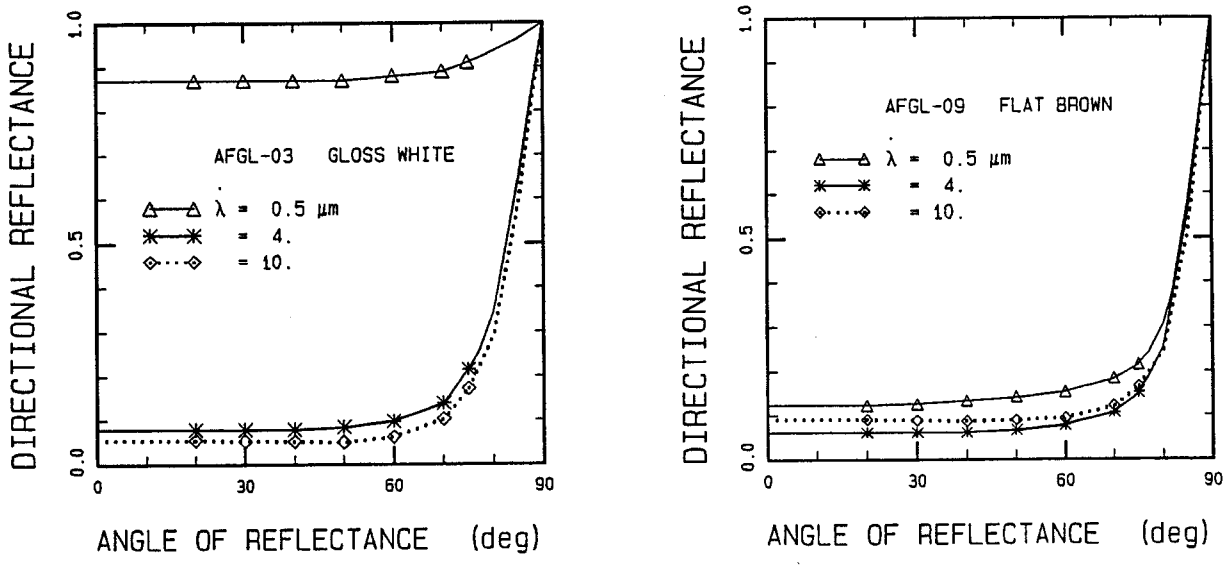

Figure 5. The Directional Reflectance at θ_i =20° for Samples AFGL-03 and -09.

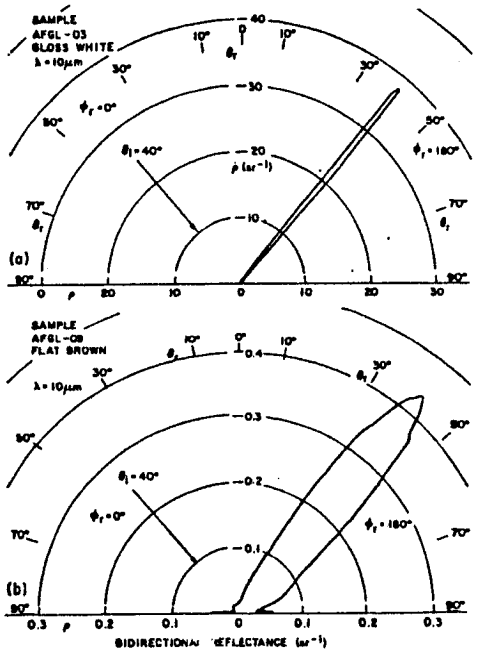

Figure 6. Linear Polar Plots of the BRDF at θ_i=40° for Samples AFGL-03 and -09

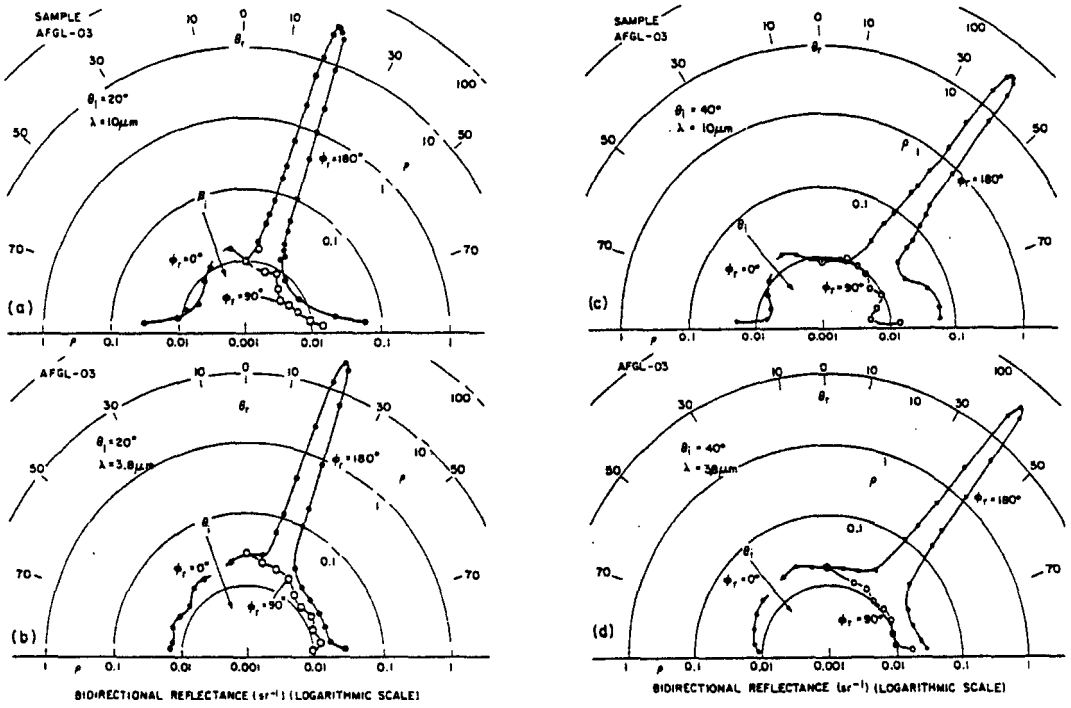

Figure 7. Logarithmic Polar Plots of the BRDF for Sample AFGL-03.
(a) $\theta_i = 20^o$, $\lambda = 10$ μm, $\varphi_i = 0$, 90 and 180º (c) $\theta_i = 40^o$, $\lambda = 10$ μm, $\varphi_i = 0$, 90 and 180º
(b) $\theta_i = 20^o$, $\lambda = 3.8$ μm, $\varphi_i = 0$, 90 and 180º (d) $\theta_i = 40^o$, $\lambda = 3.8$ μm, $\varphi_i = 0$, 90 and 180º

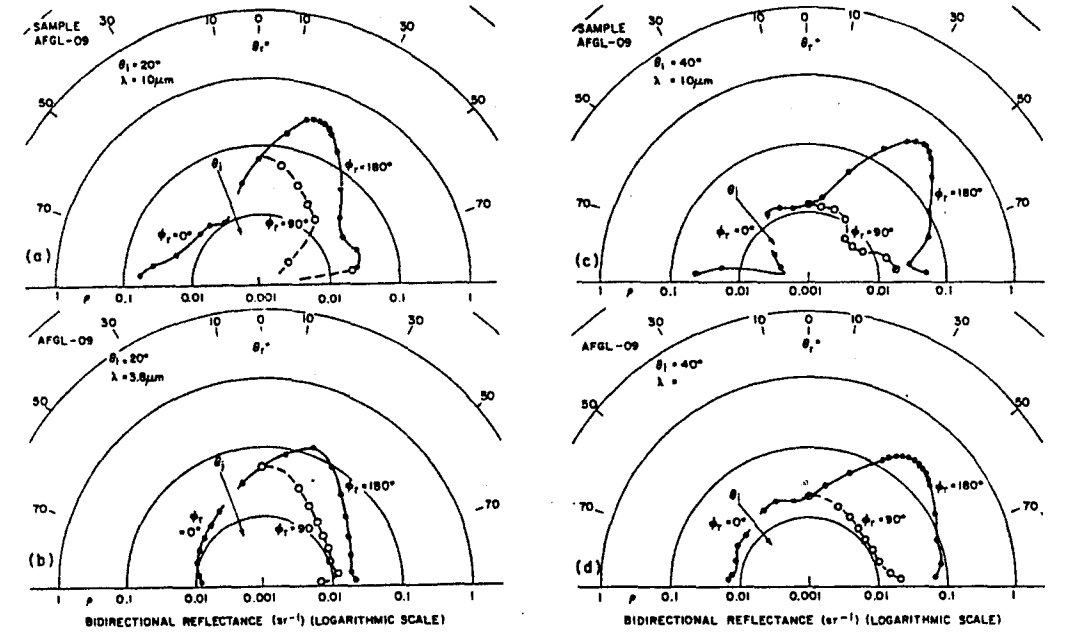

Figure 8. Polar Plots of the BRDF for Sample AFGL-09.
(a) $\theta_i = 20^o$, $\lambda = 10$ μm, $\varphi_i = 0$, 90 and 180º (c) $\theta_i = 40^o$, $\lambda = 10$ μm, $\varphi_i = 0$, 90 and 180º
(b) $\theta_i = 20^o$, $\lambda = 3.8$ μm, $\varphi_i = 0$, 90 and 180º (d) $\theta_i = 40^o$, $\lambda = 3.8$ μm, $\varphi_i = 0$, 90 and 180º

4. ROBERTSON-SANDFORD REFLECTANCE MODEL

The Robertson-Sandford (R-S) directional reflectance model provides a consistent description of surface emissive and reflectance properties in terms of a few semi-empirical parameters. Although this discussion is based on opaque planar surfaces, the model is easily extended to transmitting surfaces, by defining a spectral transmittance as part of the paint data file. Two key features of the model are a semi-empirical formulation for the angular dependence of diffuse scatter and emission, and a finite width to the angular distribution for specular scatter. The width of the specular lobe is based on a model for surface roughness developed by Trowbridge and Reitz.[8]

The R-S model is empirical in that its emittance and reflectance parameters are derived from analysis of reflectance data. Surface reflectance results from many underlying physical parameters and processes; examples are the dielectric properties of the scattering surface (expressed as the complex index of refraction), surface roughness effects, subsurface (or volume) scattering, thickness of a paint layer, scattering from a substrate, and polarization effects.[1,5,8,10-12] In addition one has to consider the combined effects of aging and weather for surfaces used on aircraft or other operational vehicles. The object of this model is to arrive at a simplified parameterization of a paint's reflectance properties that is suitable for incorporation into a code for calculating target signatures. This includes scattered sunshine, earthshine, and skyshine plus surface emissions.

The four basic parameters are:

$\rho_D(\lambda)$ = diffuse spectral reflectance,

$\varepsilon(\lambda)$ = spectral emissivity,

b = grazing angle reflectivity, and

e = width of specular lobe

The first two vary with wavelength; the second two are used to fit the angular distribution of the data. The model is empirically based in that these emittance and reflectance parameters are derived from analysis of reflectance data (e.g., those taken by SOC).

We make the physically reasonable assumption that b and e vary slowly with wavelength, so that they can be treated as constant over finite wavelength regions. For the BRDF and related quantities,

$$f_r(\theta_i, \phi_i; \theta_r, \phi_r; \lambda) = f_r(\theta_i, \phi_i; \theta_r, \phi_r)\,\rho(\lambda) = f_r\,\rho(\lambda) \quad , \tag{7}$$

where ρ_r (the BRDF) gives the angular dependence of the reflected radiation. Factorization is assumed so that the spectral and angular properties vary independently.

4.1 Model Assumptions and Properties

4.1.1 Factorization of Angular and Spectral Dependencies

The angular dependence of the emissivity and the reflectivity is essentially wavelength independent over fairly wide spectral regions.

4.1.2 Angular Dependence of Emissivity

The directional and spectral dependence of the emissivity is given by

$$\epsilon(\lambda,\theta) = \epsilon(\lambda)\frac{g(\theta)}{G(b)} \quad , \tag{8}$$

where

$$g(\theta) = \frac{1}{1 + b^2 \tan^2\theta} \quad . \tag{9}$$

By requiring ε(λ) to be the total hemispherical emittance of the surface element, G(b), the normalization constant for the angular distribution, is given by

$$G(b) = \frac{1}{\pi}\int_0^{\pi/2} \sin\theta d\theta \int_0^{2\pi} d\phi \frac{\cos\theta}{1 + b^2\tan^2\theta}$$

$$= \frac{1}{1 - b^2}\left[1 - \frac{b^2}{1 - b^2}\log(1/b^2)\right] \quad . \tag{10}$$

The cosine factor gives the effective area of the surface element. The constant b is empirical, is determined from surface reflectance data, and takes the emissivity to zero as θ_r approaches 90°. A Lambertain surface has b = 0. and emits equally in all directions.

4.1.3 Total Reflectance

Consider an incident, well collimated beam of light like that coming from the sun. From Equation (4) the amount of energy in a wavelength interval absorbed by a surface equals the emissivity of the surface. The reflected radiation is divided into diffuse and specular components, so that

$$f_r(\theta_i, \phi_i; \bar{\pi}/\bar{2}, \bar{2\pi}) = \rho_s(\theta_i) + \rho_d(\theta_i) = 1 - \epsilon(\lambda, \theta_i) \quad , \tag{11}$$

where the subscripts identify the specular and diffuse contributions and the bar indicates integration over all reflection directions (i.e., the total reflectance). Figure 9 shows the angular dependence of the total reflectance predicted by Equation (11) for three illustrative values of b.

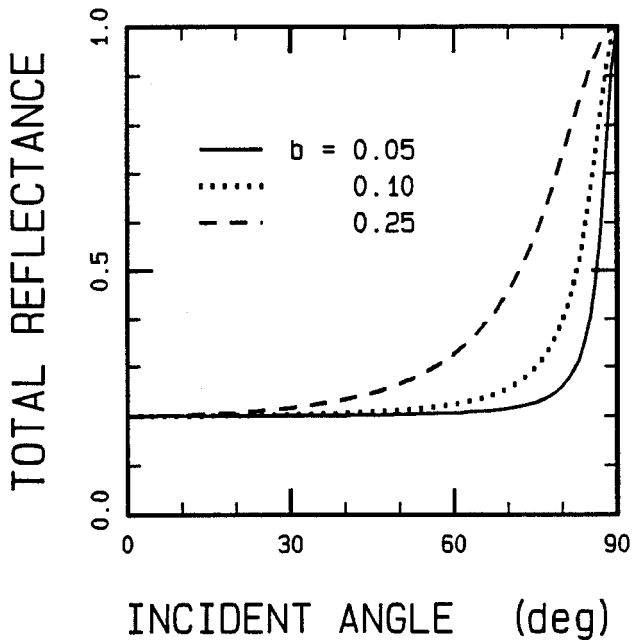

Figure 9. Angular Dependence of the Total Reflectance for Three Values of the Parameter b.

4.2 Diffuse Reflectance

Diffuse reflectance is assumed to be an average property of the surface resulting from subsurface scattering and from multiple scattering due to surface roughness on the microscopic level. The amount of radiation available for diffuse scattering varies with the angle of the incident beam. We assume that

the directional dependence from an illuminated surface is the same as its emissivity. We then assume that the scattering process is symmetrical, e.g.,[6]

$$f_r(\theta_i, \phi_i; \theta_r, \phi_r) = f_r(\theta_r, \phi_r; \theta_i, \phi_i) \quad , \tag{12}$$

and that the diffuse BRDF is given by

$$f_d(\theta_i, \phi_i; \theta_r, \phi_r) = \frac{1}{\pi} g(\theta_r)\, \rho_d(\lambda)\, g(\theta_i) / [G(b)]^2 \quad . \tag{13}$$

The amount of diffusely scattered energy is given by $\rho_d(\lambda)g(\theta_i)$, and the angular distribution of that radiation is given by $g(\theta_r)$. The diffusely scattered energy is given by

$$I_d(\theta_i, \theta_r) = \frac{1}{\pi} (E_{inc} \cos\theta_i)\, f_d(\theta_i, \phi_i; \theta_r, \phi_r) \quad . \tag{14}$$

4.3 Specular Reflectance

A modified form of a model developed by Trowbridge and Reitz[8] is used to calculate the specular reflection. They showed that the optical properties of a rough surface can be described by an equivalent circular ellipsoid with eccentricity e. This parameter e is the parameter in our model that describes the angular width of the specular lobe. The width of the angular distribution for specular scattering is due to single scattering from the curved elliptical surface. A finite surface element is composed of many micro-elliptical surfaces. The function $h(\alpha)$ is the surface structure function. The BRDF is given by

$$f_s(\theta_i, \phi_i; \theta_r, \phi_r) = \frac{1}{4\pi} \rho_s(\lambda, \theta_i) \frac{h(\alpha)}{H(\theta_i)} \frac{1}{\cos\theta_r} \tag{15}$$

$$h(\alpha) = \frac{1}{[e^2 \cos^2\alpha + \sin^2\alpha]^2} \quad , \tag{16}$$

where α is the angle between the glint vector ($\hat{g}$) and surface normal, and $\cos\alpha = \hat{g} \cdot \hat{n}$.

Trowbridge and Reitz define $\rho_s(\lambda, \theta_s)$ as the Fresnel reflection coefficient for scattering at an angle θ_s for the refraction and absorption indices n and k of a dielectric surface. Here, the total specular reflection coefficient, $\rho_s(\lambda, \theta_i)$, is used for the angle θ_i as defined by

$$\rho_s(\lambda, \theta_i) = 1 - \rho_d(\lambda, \theta_i) - \epsilon(\lambda, \theta_i) \quad . \tag{17}$$

Since $\rho_s(\theta_i)$ gives the fraction of the incident energy which undergoes specular reflection, it is required that the integral of Equation (15) over all observer angles (θ_r,φ_r) be normalized to ρ_s. Thus,

$$H(\Theta_i) = \frac{1}{4\pi}\int d\Omega_r h(\alpha) = \frac{1}{2e^2}\{(1 - e^2)Cos\Theta + [2e^2 + (1-e^2)^2Cos^2\Theta]/\sqrt{(1 - e^2)^2Cos^2\Theta + 4e^2}\} \quad . \tag{18}$$

The energy scattered specularly for given incident and exciting directions is

$$I_s(\Theta_i;\Theta_r) = (E_{inc}Cos\Theta_i)\, f_s(\Theta_i,\phi_i;\Theta_r,\phi_r)\, A\, Cos\Theta_r$$

$$= (E_{inc}Cos\Theta_i)\frac{\rho_s(\Theta_i)}{4\pi}\frac{h(\alpha)}{H(\Theta_i)}\, A \quad . \tag{19}$$

Maximum specular scatter occurs when $\alpha = 0$.

An example of specular scattering for three different values of the parameter e is shown in Figure 10. The BRDF is calculated for an angle of 20° for the incident radiation and for a total reflectivity (specular only) of 0.20.

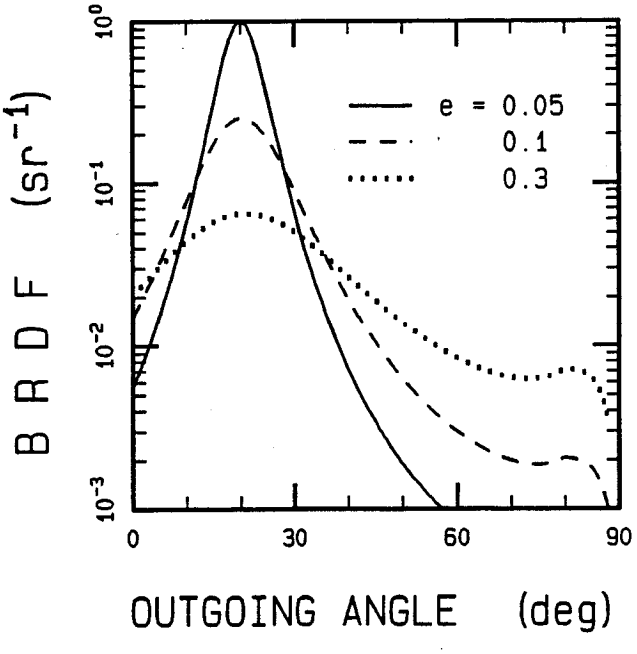

Figure 10. The BRDF for Incident Radiation at 20° and for Three Values of the Parameter e.

4.4 Shadowing and Obscuration

As the observer angle θ_r approaches 90°, the predicted amount of specularly reflected energy remains finite. This leads to divergences in the BRDF as θ approaches 90°. The data shown by Torrence and Sparrow exhibit this divergence, but with a sharp cut-off at 90° so that there is a peak in the BRDF around 85° [11] The divergence in the BRDF arises from the parameterization of the surface roughness as a single equivalent curved surface (ellipsoidal) that scatters for all angles. Shadowing and obscuration of scattering surface elements occur for grazing angles because the surface is planar in the macroscopic sense; this causes a cut-off at 90°. Convenient cut-off factors are

$$d(\Theta) = \frac{1}{1 + \delta Tan\Theta} , \qquad (20)$$

and

$$d(\Theta) = \frac{1}{1+\delta^2 Tan^2\Theta} . \qquad (21)$$

Both factors lead to very messy normalization integrals when combined with the specular scattering function, Equation (16). One way to get around this is to note that the cut-off is only significant in the 80-90° range and that Equation (16) is approximately constant except for incident angles near 90°. Equation (21) is used in this model to cut-off the BRDF with δ = b and normalized to 1.0 at θ = 80°.

4.5 Comparison to SOC Data

Comparisons to reflectance data are presented for two samples, AFGL-01 (Camouflage Paint) at 4.0 μm and AFGL-10 (Gloss White Paint) at 3.0 μm. The model parameters used for each sample are given in Table 4. Figure 11 shows a comparison of the BRDF for AFGL-01 at a wavelength of 3.8 μm and at three angles of incidence (θ_i = 20, 40, 60°) for forward scatter, φ_r = 180°; this shows the glint lobe. The angular dependencies of the total reflectance for AFGL-01 and AFGL-10 are shown in Figures 12 and 14, respectively. Similar comparisons of the BRDF for sample AFGL-10 are shown in Figure 13. The model does a good job of following the trends in the angular dependence of the data. The sharper specular features seen in Sample AFGL-10 (White Gloss Paint) result from a smaller value of e (see Table 4). The calculations for each sample were done with fixed values of the four parameters, b, e, ε_o, and ρ_D, showing that this simple four-parameter model gives a good fit to the data.

Table 4. Parameters for Reflectance Model at 4μm.

Paint Sample	ρ_0	ε_0	b	e
AFGL-01 (Camouflage)	.07	.85	.12	.12
AFGL-10 (White Gloss)	.05	.88	.08	.012

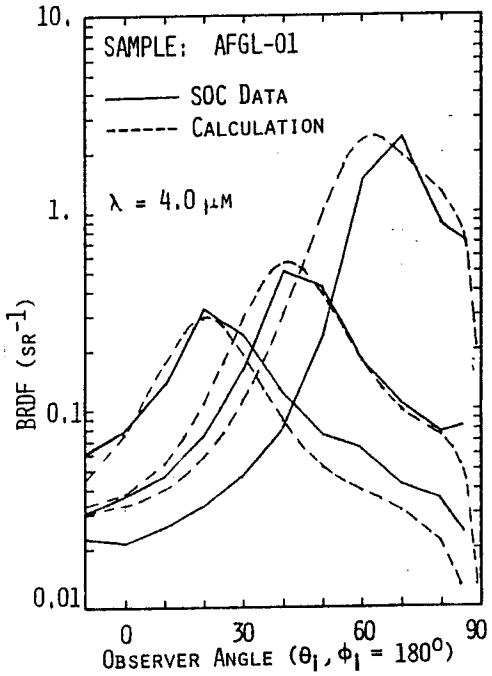

Figure 11. Comparison of Model Calculations (- - -) and SOC Data (——) at 4 μm for sample AFGL-01 for Three BRDF (θ_i = 20, 40, 60°).

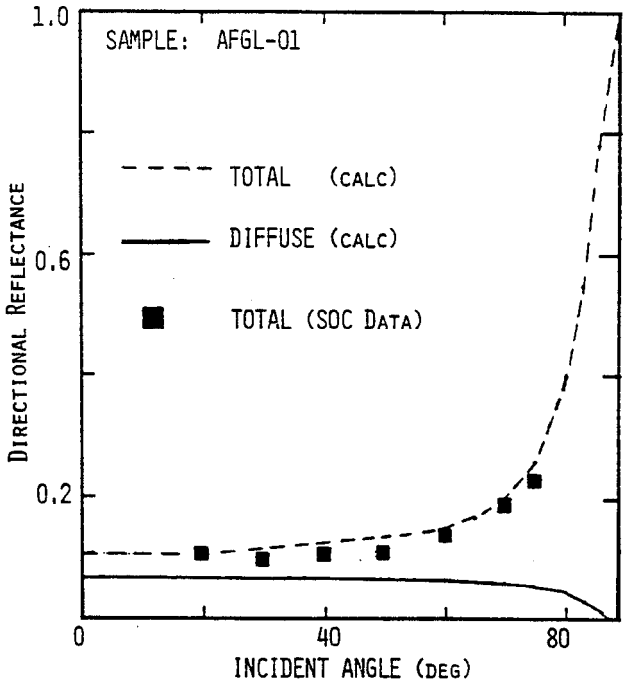

Figure 12. Model Calculations of the Total and Diffuse Reflectance and the SOC Reflectance Data at 4.0 μm for AFGL-01.

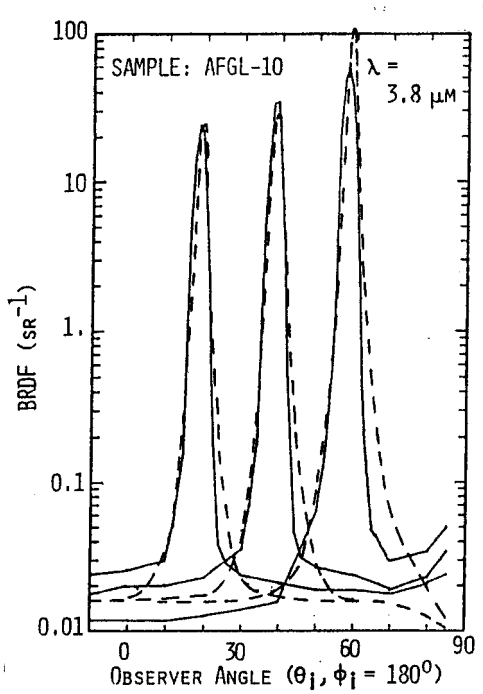

Figure 13. Comparison of Model Calculations (- - -) and SOC Data (——) at 3.8 μm for sample AFGL-10 for BRDF (θ_i = 20, 40, 60°).

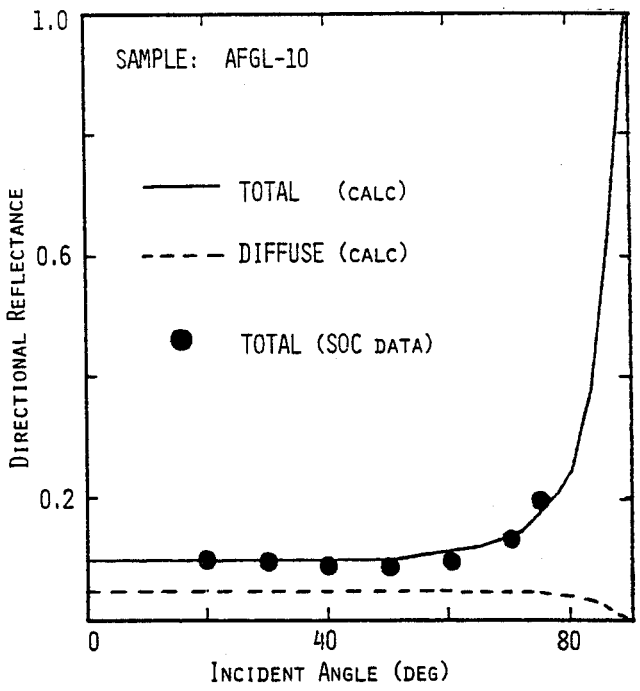

Figure 14. Model Calculations of the Total and Diffuse Reflectance and the SOC Data at 4.0 μm for Sample AFGL-10.

5. CONCLUSIONS

As IR detection systems continue to become increasingly sophisticated, the reflectance properties of airframe paints are one of many signature elements to which aircraft designers must become increasingly sensitive. Our goal in this paper has been to make the research community aware of the reflectance (and aircraft IR signature) data available at PL/GPOA and to introduce an approach for synthesizing these data within the framework of an IR signature model. Further work to expand the data base, analyze the reflectance data, and further validate the model is continuing (and support is welcome!).

6. REFERENCES

1. J. T. Neu and R. S. Dummer, "Theoretical and Practical Implication of the Bidirectional Reflectance of Spacecraft Surfaces", AIAA Journal, 7, 484 (1969).

2. J. T. Neu, R. S. Dummer, and J. H. Wray, Private Communication to B. Sandford (1982).

3. J. T. Neu, R. S. Dummer, M. Beecroft, P. McKenna, and D. C. Robertson, "Surface Optical Property Measurements on Bark and Leaf Samples", Phillips Laboratory Rpt. PL-TR-91-2009 (December 1990) ADA240714.

4. D. C. Robertson, "Aircraft Contrast Signatures in the Infrared Spectral Region", SPIE, 327, 59 (1982).

5. W. L. Wolf and Zissis, eds., The Infrared Handbook, The IRIA Center, Environmental Research Institute of Michigan, P.O. Box 8618, Ann Arbor, MI (1978).

6. F. E. Nicodemus, J. C. Richmond, J. J. Hsia, I. W. Ginsberg, and T. Limperis, "Geometrical Considerations and Nomenclature for Reflectance", U. S. Department of Commerce, National Bureau of Standards, Washington, DC, NBS Monograph 160 (1977).

7. F. E. Nicodemus, "Directional Reflectance and Emissivity of an Opaque Surface", Appl. Opt., 4, 767 (1965).

8. T. S. Trowbridge and K. P. Reitz, "Average Irregularity of a Rough Surface for Ray Reflections", J. Opt. Soc. Am., 65, 531 (1975).

9. D. Tanre, et al., "Atmospheric Modeling for Space Measurements of Ground Reflectances, Including Bidirectional Properties", Appl. Opt., 18, 3587 (1979).

10. J. R. Aronson and A. E. Emslie, "Modeling the Infrared Emittance of Paints", Report No. 83670-28, Arthur D. Little, Inc., Cambridge, MA 02140 (October 1980).

11. K. E. Torrance and E. M. Sparrow, "Theory for Off-Specular Reflection from Roughened Surfaces", J. Opt. Soc. Am., 67, 1105 (1967).

12. J. C. Leader, "Analysis and Prediction of Laser Scattering from Rough-Surface Materials", J. Opt. Soc. Am., 69, 610 (1979).